SUPPORTING INFORMATION FOR

Influence of Symmetry on Magneto-Optical properties of a Macrocycle Dy^{III} Complex

Yolimar Gil[a*], Ricardo Costa de Santana[b], Andrés Vega[c], Daniel Aravena[d*], Evgenia Spodine[a].

[a] *Facultad de Ciencias Químicas y Farmacéuticas, Universidad de Chile, Olivos 1007, 8380544, Santiago, Chile.*
[b]*Instituto de Física, Universidade Federal de Goiás, Campus Samambaia, 74690-900, Goiânia (GO), Brazil.*
[c]*Departamento de Ciencias Químicas, Universidad Andrés Bello, Santiago, Chile*
[d]*Departamento de Química de los Materiales, Facultad de Química y Biología, Universidad de Santiago de Chile, Casilla 40, Correo 33, Santiago, Chile.*

Table of contents

I. Synthesis and characterization

$[Dy(L^{Pr})(NO_3)_2]\cdot(H_2O)\cdot(NO_3)$ (**1**) was synthesized following a similar procedure previously reported [1]. A solution of $Dy(NO_3)_3\cdot 5H_2O$ (0.5 mmol) in 30 ml of acetonitrile was added with stirring to a solution of 2,6-pyridinedicarboxaldehyde (135 mg, 1mmol) in 50 mL of the same solvent. Then, a solution of 1,3-diaminepropane (1 mmol) in 50 ml acetonitrile was added. The mixture was stirred for 4 h at room temperature. Pale amber block crystals were obtained by slow evaporation of the solutions after five weeks. Yield 0.138 g (38.7 %). Anal. calc. For: C20H24DyN9O10: C, 33.69; H, 3.39; N, 17.68 %. Found C, 33.74; H, 3.55; N, 17.37 %. IR (cm^{-1}): 2962, 2870 (m, C-H), 1645 (m, C=N, imine), 1595 (m, C=N, py), 1456 and1297 (s, NO_2, bidentate nitrate), 1380 (m, NO_2, nitrate anion) (Figure S1).

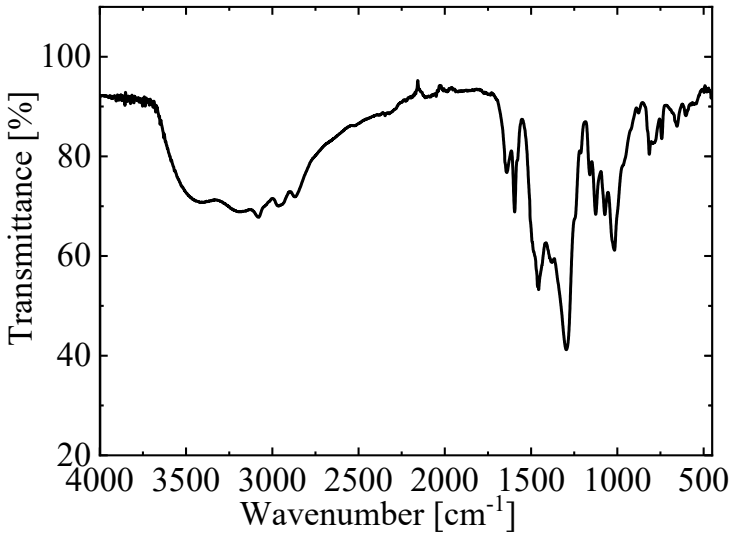

Figure S1. FTIR spectrum for **1**.

II. X-ray crystallography

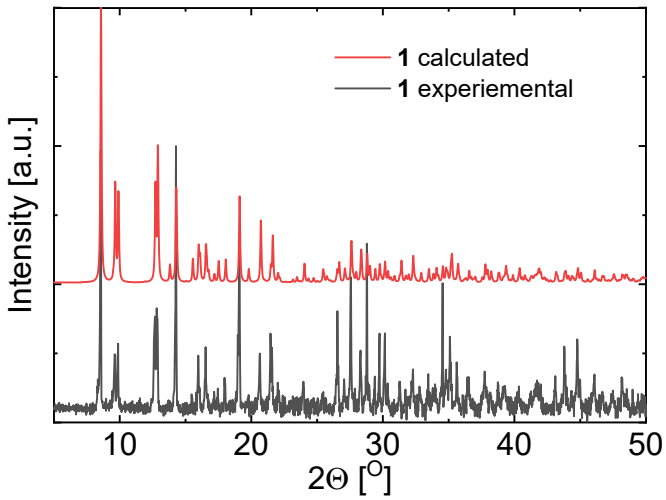

Figure S2. Comparison between experimental and calculated powder X-ray diffraction (PXRD) patterns for **1**.

Table S1. Crystal data and structure refinement details for **1**.

	1
Chemical formula	$C_{20}H_{24}DyN_9O_{10}$
M_r	712.98
Cr. Syst.	Monoclinic
Space gr.	$P2_1/c$
a (Å), b (Å), c (Å)	13.4207(18),18.561(3), 11.3906(15)
α (°), β (°), γ (°)	90, 112.650(2), 90
V (Å^3)	2618.6(7)
Z	4
Radiation	Mo K_α
μ (mm^{-1})	2.925
Crystal size (mm)	0.08 × 0.09 × 0.12
T_{min}, T_{max}	0.789, 0.968
Total, unique, observed data [I > 2σ(I)]	20158, 5129, 4447
R_{int}	0.029
R, wR, S	0.0204, 0.0481, 1.03
N. Ref, N. Par	5129, 370
$\Delta\rho_{max}$, $\Delta\rho_{min}$ (e Å^{-3})	-0.61, 1.00

Table S2. Selected bond distances (Å) and angles (°) for **1**.

Dy1 -N1	2.553(2)	O5 -N8	1.264(3)
Dy1 -N2	2.563(3)	N1 -C1	1.333(4)
Dy1 -N3	2.562(2)	N1 -C5	1.342(4)
Dy1 -N4	2.580(2)	N2 -C6	1.265(4)
Dy1 -N5	2.579(3)	N2 -C7	1.464(4)
Dy1 -N6	2.529(2)	N3 -C9	1.471(5)
Dy1 -O1	2.499(2)	N3 -C10	1.269(4)
Dy1 -O2	2.472(2)	N4 -C11	1.335(4)
Dy1 -O4	2.452(2)	N4 -C15	1.336(4)
Dy1 -O5	2.482(2)	N5 -C16	1.267(4)
O1 -N7	1.265(3)	N5 -C17	1.463(4)
O2 -N7	1.269(3)	N6 -C19	1.467(4)
O4 -N8	1.262(3)	N6 -C20	1.272(4)
O1 -Dy1 -O2	51.37(7)	N2 -Dy1 -N3	67.33(8)
O1 -Dy1 -O4	135.71(7)	N2 -Dy1 -N4	115.85(8)
O1 -Dy1 -O5	156.99(8)	N2 -Dy1 -N5	143.54(8)
O2 -Dy1 -O4	150.47(8)	N2 -Dy1 -N6	125.75(7)
O2 -Dy1 -O5	137.17(7)	N3 -Dy1 -N4	62.37(8)
N1 -Dy1 -N2	62.58(7)	N3 -Dy1 -N5	124.84(7)
N1 -Dy1 -N3	116.84(8)	N3 -Dy1 -N6	143.63(8)
N1 -Dy1 -N4	178.33(8)	N4 -Dy1 -N5	62.48(8)
N1 -Dy1 -N5	118.32(7)	N4 -Dy1 -N6	118.39(8)
N1 -Dy1 -N6	63.18(8)	N5 -Dy1 -N6	67.68(8)

Table S3. Continuous Shape Measurement calculations (CShM) of the first coordination sphere of **1**, referring to all standard 10 vertices of the polyhedron.

Polyhedron, ML10	**1**
Planar decagon	34.671
Enneagonal pyramid	24.229
Octagonal bipyramid	14.903
Pentagonal prism	13.136
Pentagonal antiprism	12.289

Bicapped cube J15	9.518
Bicapped square antiprism J17	3.387
Metabidiminished icosahedron J62	7.016
Augmented tridiminished icosahedron J64	19.874
Sphenocorona J87	**3.204**
Staggered Dodecahedron (2:6:2)	5.155
Tetradecahedron (2:6:2)	3.825
Hexadecahedron (2:6:2) or (1:4:4:1)	6.757

III. Magnetic characterization

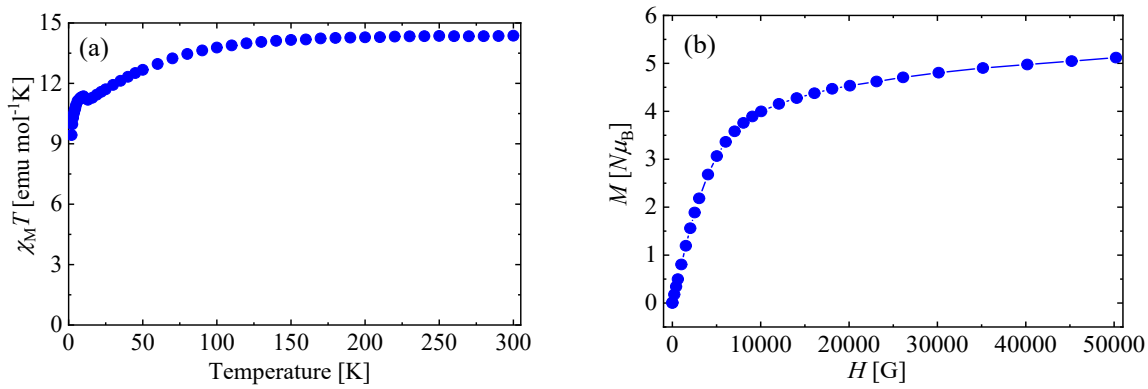

Figure S3. (a) Temperature dependence of the product χ_MT with an applied field of 3 KOe. (b) Molar magnetization as a function of applied magnetic field at 2 K for **1**.

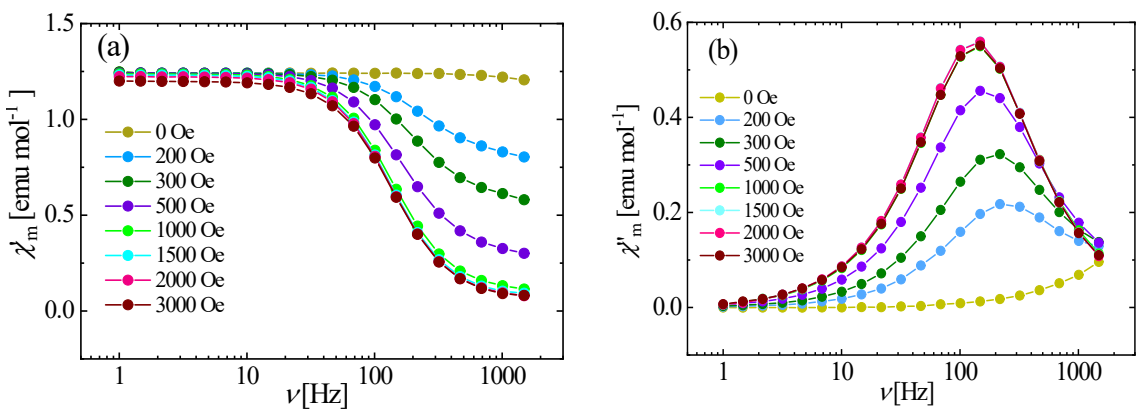

Figure S4. Dependence of the in-(left) and out-of-phase (right) susceptibility with the frequency at different static fields at 8K for **1**.

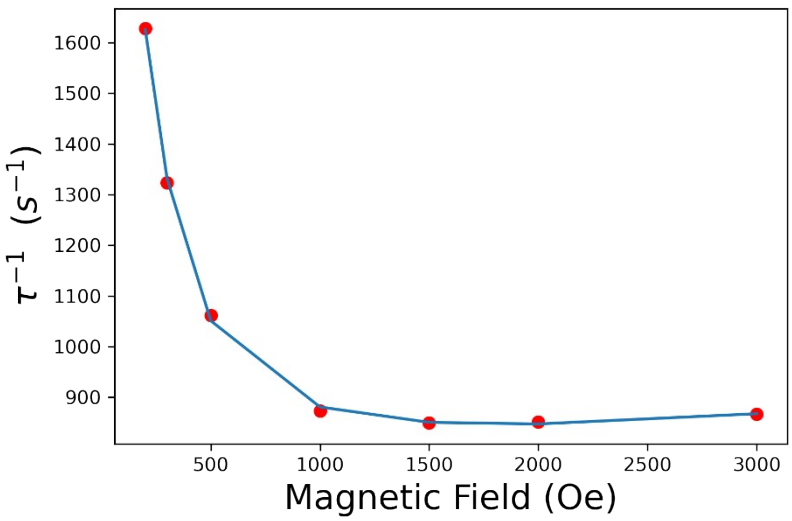

Figure S5. Field dependence of the relaxation time for 1 at 8K. Data were fitted to $\tau^{-1} = AH^2 + \frac{B_1}{1 + B_2H^2} + D$ with parameters A = 6.04 x 10^{-6} $Oe^{-2}s^{-1}$; B_1 = 1.49 x 10^3 s^{-1}; B_2 = 2.04 x 10^{-5} Oe^{-2}; D = 805.1 s^{-1}.

Table S4. Parameters from the fit of Cole-Cole plots for **1**.

T (K)	χ_S	χ_T	**τ**	α
4.10	1.66E-01	2.90	2.06E-01	2.11E-01
4.40	1.64E-01	2.38	8.96E-02	1.34E-01
4.70	1.58E-01	2.14	4.94E-02	9.47E-02
5.00	1.50E-01	1.98	3.00E-02	7.09E-02
5.30	1.43E-01	1.86	1.91E-02	5.58E-02
5.60	1.37E-01	1.75	1.27E-02	4.50E-02
5.90	1.31E-01	1.66	8.72E-03	3.75E-02
6.20	1.26E-01	1.59	6.15E-03	3.21E-02
6.50	1.22E-01	1.51	4.45E-03	2.75E-02
6.80	1.18E-01	1.45	3.28E-03	2.48E-02
7.10	1.15E-01	1.39	2.46E-03	2.15E-02
7.40	1.10E-01	1.34	1.88E-03	2.07E-02
7.80	1.07E-01	1.27	1.34E-03	1.82E-02
8.20	1.04E-01	1.21	9.81E-04	1.64E-02
8.60	1.01E-01	1.16	7.29E-04	1.49E-02
9.00	9.95E-02	1.11	5.51E-04	1.38E-02
9.40	9.66E-02	1.06	4.22E-04	1.36E-02
9.80	9.79E-02	1.02	3.29E-04	1.17E-02

10.30	9.61E-02	9.75E-01	2.43E-04	1.01E-02
10.75	9.62E-02	9.32E-01	1.82E-04	1.05E-02
11.20	9.78E-02	8.91E-01	1.36E-04	8.99E-03
11.70	1.04E-01	8.54E-01	1.03E-04	7.85E-03
12.30	1.09E-01	8.07E-01	6.86E-05	1.29E-02
12.90	1.38E-01	7.71E-01	5.08E-05	1.01E-02
13.50	1.94E-01	7.39E-01	3.91E-05	9.60E-03
14.10	2.22E-01	7.10E-01	2.76E-05	2.70E-02
15.00	3.49E-01	6.70E-01	2.08E-05	4.28E-02

IV. Magneto-structural correlation

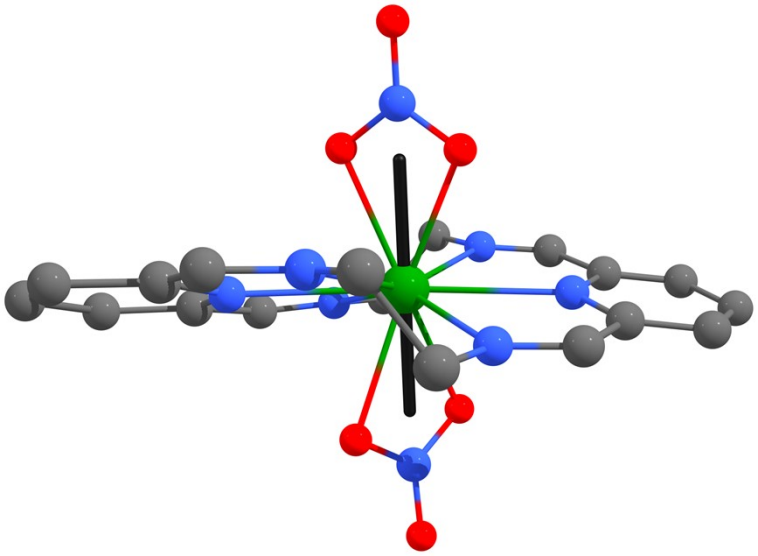

Figure S6. Calculated orientation of the main magnetic axis of the ground Kramers doublet for $[Dy(L^{N6})(NO_3)_2](BPh_4)$[2].

V. Optical characterization

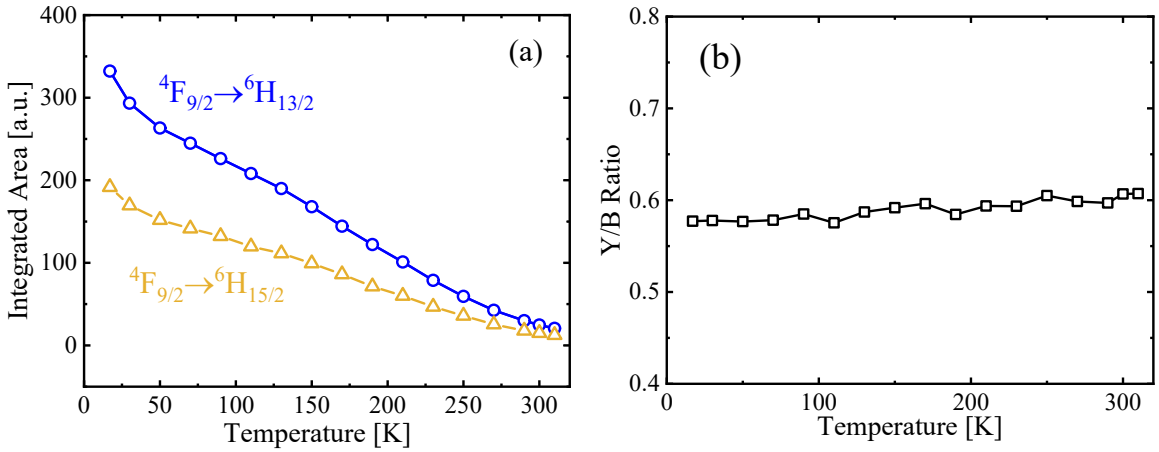

Figure S7. Thermal variation of (a) the integrated area of luminescence intensities for **1** for $^4F_{9/2} \rightarrow {}^6H_{15/2}$ (blue, B) and $^4F_{9/2} \rightarrow {}^6H_{13/2}$ (yellow, Y) transitions, and (b) of the Y/B ratio.

Table S5. CIE (x,y) coordinates and CCT (K) values for all complexes.

T(K)	CIE (x;y)	CCT(K)
310	0.278, 0.314	9080
17	0.293, 0.348	7383

VI. References

1 P. Fuentealba, D. Villagra, Y. Gil, H. Aguilar-Bolados, Prof. R. C. de Santana, G. Gasparotto, A. Vega, J. Manzur and E. Spodine, *Eur. J. Inorg. Chem.*, 2021, **25**, 4543–4551.

2 P. Y. Liao, Y. Liu, Z. Y. Ruan, H. L. Wang, C. G. Shi, W. Deng, S. G. Wu, J. H. Jia and M. L. Tong, *Inorg. Chem.*, 2023, **62**, 1075–1085.